Equilibrium Switching in Nonlinear Interaction Networks with Concurrent Antagonism

Jomar F. Rabajante[a,b,*]

[a] *Institute of Mathematics, University of the Philippines Diliman, Quezon City, Philippines*
[b] *Institute of Mathematical Sciences and Physics, University of the Philippines Los Baños, Laguna, Philippines.*

Abstract

NOTE: This is an early preprint version only.

In this paper, we examine a nonlinear concurrent decision-making model (CDM) of interaction networks that involve more than two antagonistic components (e.g., proteins, species, communities, mental choices). The model assumes sigmoid kinetics where every component stimulates itself but represses all others. We are able to prove general dynamical properties of the CDM (e.g., location and stability of steady states) for any dimension of the state space even if the reciprocal antagonism between two components is asymmetric. There are cases where asymmetric interaction generates oscillatory behavior. Some parameters can serve as biological regulators for inducing steady state switching by leading a temporal state to escape an undesired equilibrium. Increasing the maximal growth rate and decreasing the decay rate can expand the basin of attraction of a steady state with the desired component having the dominant value. We further show that perpetually adding an external stimulus can shutdown multi-stability of the system that increases the robustness of the system against stochastic noise.

Keywords: biological switch, regulatory network, species competition, sigmoid kinetics, multi-stability, repressilator

2000 MSC: 34C60, 92B05

PACS: 87.10.Ed, 87.18.Cf

Highlights

1. Mathematical properties of n-dimensional concurrent decision-making ODE model.
2. Intuitive graphical technique for component-wise and steady state stability analysis.

*Corresponding author. Phone number: +63 49 536-6610. Present address: Graduate School of Science and Technology, Shizuoka University, 3-5-1 Johoku, Naka-ku, Hamamatsu City, 432-8561 Japan.

Email address: jfrabajante@upd.edu.ph (Jomar F. Rabajante)

3. Search for parameter conditions that control steady state switching.

4. Illustrations of multi-stable systems and repressilators.

Graphical Abstract

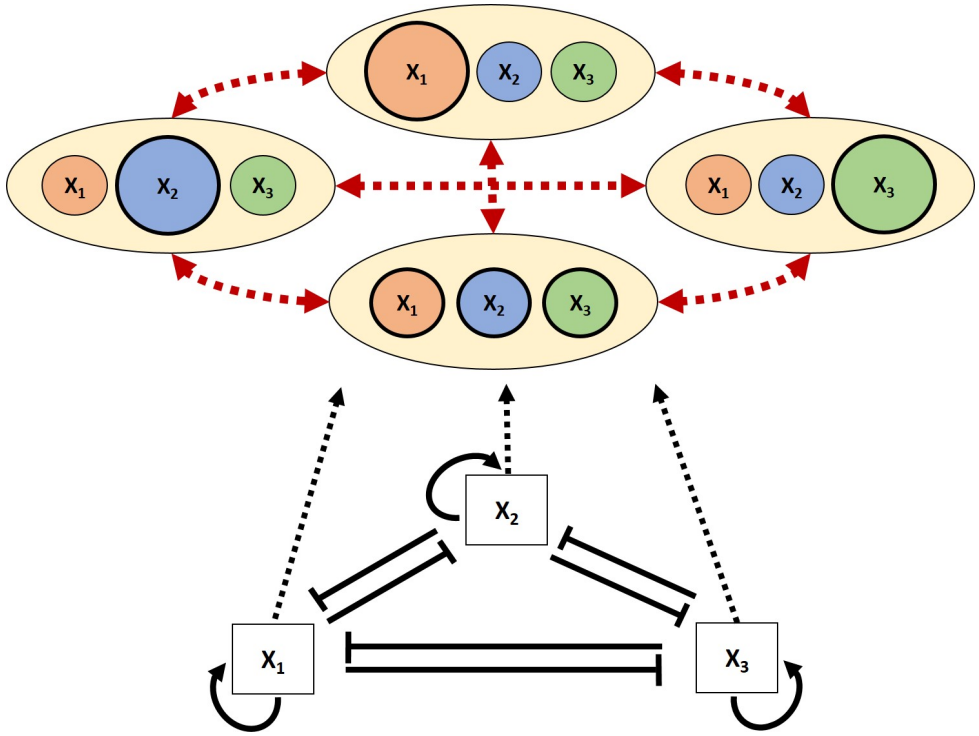

1. Introduction

Mathematical analysis of interaction networks are valuable in understanding the dynamics of complex systems [1, 2, 3, 4, 5]. Concurrent antagonism, where every component of the system simultaneously represses each other, is one of the interaction systems that commonly occurs in nature. This type of interaction can be observed from gene regulation [6, 7, 8, 9, 10, 11] to mental perception and community structures [12, 13, 14, 15, 16]. The concurrent decision-making model (CDM), which was originally proposed by Cinquin and Demongeot [17], represents the mutual antagonistic interaction among components. The characteristics (e.g., initial condition, growth, decay and strength of inhibition) of each component and the inter-component interaction mechanism of the CDM decide what component eventually dominates the system [18, 19, 20].

In this paper, we study the mathematical properties of the CDM where a component of the system can denote any inhibiting factor (e.g., protein, species, community, mental choice) as long

PeerJ PrePrints | http://dx.doi.org/10.7287/peerj.preprints.382v1 | CC-BY 4.0 Open Access | received: 8 May 2014, published: 8 May 2014

as the interaction among the components follows the network shown in Figure (1). We assume that each component stimulates itself and the kinetics describing its progression is sigmoidal. This non-polynomial progression curve is an alternative to the generic polynomial models (e.g., Lotka-Volterra), especially when polynomial models cannot replicate the effect of sigmoidal growth [21, 14, 22, 23, 24, 25]. We can regard the self-stimulation rate in the CDM model as a characteristic of individuals or populations for increasing fitness and avoiding extinction. Furthermore, the CDM with sigmoid growth rate can be a candidate model of biological switches that exhibit multi-stability (co-existence of multiple stable equilibria) [26, 27, 28, 29]. Self-stimulation is a common property of master switches in gene regulation and other biological signaling systems [30, 17, 31, 32].

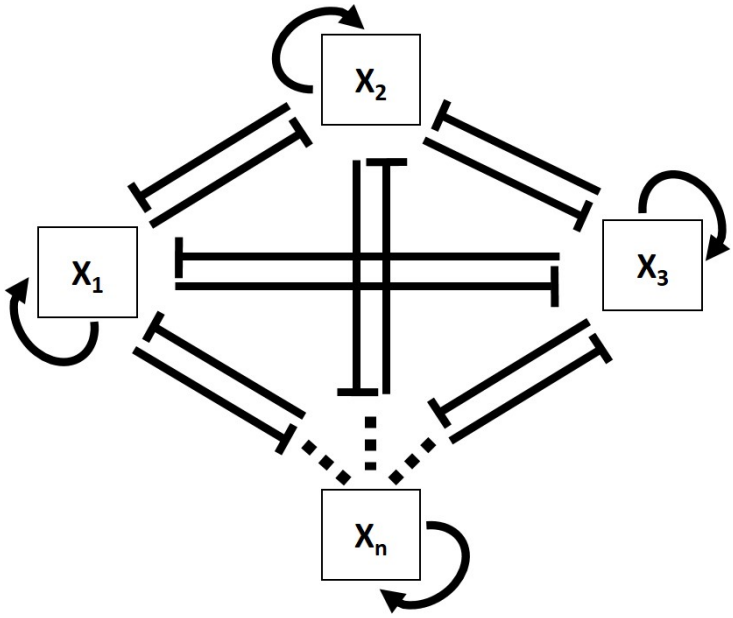

Figure 1: CDM interaction network (adopted from [33, 17]). Bars represent inhibition, while arrows represent stimulation. The nodes represent interacting components of a system.

The CDM can be used to study various large networks by converting them to coarse-grained phenomenological networks with auto-activation loops and concurrent antagonism among modules of sub-networks. The coarse-grained network in CDM format can be a motif that is part of a much larger network [34, 35, 36, 37, 38, 39]. The qualitative behavior of the dynamics of the CDM can be analyzed by translating the interaction network into a system of ordinary differential equations (ODE). Existing ODE models of CDM have been employed to study cell differentiation but only for symmetric interactions [40, 41, 17]. Our mathematical results are

PeerJ PrePrints | http://dx.doi.org/10.7287/peerj.preprints.382v1 | CC-BY 4.0 Open Access | received: 8 May 2014, published: 8 May 2014

generalizable for high-dimensional systems (number of components is more than two) and for asymmetric antagonism. The model that we analyze has more adjustable parameters to represent a wider range of situations and to predict more types of outcomes (e.g., multi-stable states and oscillation).

Stability and bifurcation analyses of the ODE model are performed by utilizing the geometric properties of the sigmoid kinetics. The analysis focuses on the non-negative real-valued states of the ODE model and the steady states are classified based on the structure of its components. For example, a desired steady state refers to the equilibrium point with the desired component having the dominant value. We search for parameter conditions that control equilibrium switching. Equilibrium switching means driving a solution to the ODE model to converge from one steady state to another steady state. We identify if varying the values of some parameters, such as maximal growth rate, effect of external stimuli, decay rate and interaction strength, can steer the system toward a desired equilibrium. Illustrative examples of several cases (e.g., finite and infinite number of steady states, and oscillations) are presented.

2. Model and Methods

A state $X = (X_1, X_2, ..., X_n)$ represents a temporal stage in the CDM. The component (coordinate) X_i of a state represents the value (concentration, population, estate, worth) of the i-th node in the CDM interaction network. A stable steady state $X^* = (X_1^*, X_2^*, ..., X_n^*)$ represents the long-term fate of the system for a certain set of parameter values and initial condition. For example, a steady state may represent a certain cell phenotype in the cellular differentiation process, an outcome of competition among species, a longstanding social structure in a community, or a preference from a set of choices. The dominant component dictates the expressed gene, the victorious species, the leading social class, or the prevailing choice among conflicting alternatives.

The CDM interaction network with self-stimulation (auto-activation) can be translated to an ODE model as follows:

$$\frac{dX_i}{dt} = F_i(X) = \frac{\beta_i X_i^{c_i}}{K_i + X_i^{c_i} + \sum_{j \neq i} \gamma_{i,j} X_j^{c_{i,j}}} + g_i - \rho_i X_i, \quad \text{for } i = 1, 2, ..., n \tag{1}$$

where n is the number of nodes in the network. This ODE model is a generalization of the

PeerJ PrePrints | http://dx.doi.org/10.7287/peerj.preprints.382v1 | CC-BY 4.0 Open Access | received: 8 May 2014, published: 8 May 2014

symmetric ODE model in [17]. We restrict the parameters to be non-negative real numbers. The parameter β_i is the growth constant of the unrepressed X_i relative to the first-order degradation; $\rho_i \leq 1$ is the assumed first-order degradation rate (exponential decay) of X_i; and $\gamma_{i,j}$ is the interaction coefficient associated with the inhibition of X_i by X_j. If $\gamma_{i,j} = 0$ then X_j does not inhibit the growth of X_i. The matrix of interaction coefficients $[\gamma_{i,j}]$ can be symmetric or asymmetric. Moreover, we consider

$$g_i = e_i + \alpha_i s_i \tag{2}$$

to represent constant basal or constitutive growth (e_i) of X_i [42, 43] plus the effect of the external stimulus with concentration s_i and rate α_i. In this paper, we assume that g_i is constant. By using an ODE model, we assume that the time-dependent average dynamics of the CDM is continuous in both time and state space.

We define the multivariate sigmoid function H_i by

$$H_i(X_1, X_2, ..., X_n) = \frac{\beta_i X_i^{c_i}}{K_i + X_i^{c_i} + \sum_{j \neq i} \gamma_{i,j} X_j^{c_{i,j}}} \tag{3}$$

which comes from the classical Hill equation [44, 45]. The terms $\sum_{j \neq i} \gamma_{i,j} X_j^{c_{i,j}}$ in the denominator reflect the inhibitory influence of other components on the growth of X_i. The parameter $K_i > 0$ is the threshold constant. If all $X_j = 0$ for all $j \neq i$ then the function value of H_i is equal to $\beta_i/2$ when $X_i = K_i^{1/c_i}$. The parameter $c_i \geq 1$ defines the shape and the steepness of the sigmoid curve associated with X_i, and denotes self-stimulation. The parameter $c_{i,j}$, $j \neq i$ affects the strength of inhibition of X_i by X_j. These exponents represent the nonlinear sigmoid kinetics possibly formed by multiple intrinsic and extrinsic processes affecting the growth of X_i [46]. In addition, the lower bound of H_i (3) is zero and its upper bound is β_i. Thus, the value $\beta_i + g_i$ can also be interpreted as the maximal growth rate of X_i.

2.1. Graphical technique for stability analysis

We can investigate the multivariate sigmoid function (3) by looking at the univariate function defined by

$$H_i^1(X_i) = \frac{\beta_i X_i^{c_i}}{K_i + X_i^{c_i} + \sum_{j \neq i} \gamma_{i,j} X_j^{c_{i,j}}} \tag{4}$$

where each X_j, $j \neq i$ is taken as a dynamic parameter. This means that we project the high-dimensional space onto a two-dimensional plane. If $c_i > 1$, the graph of the univariate function

PeerJ PrePrints | http://dx.doi.org/10.7287/peerj.preprints.382v1 | CC-BY 4.0 Open Access | received: 8 May 2014, published: 8 May 2014

H_i^1 in the first quadrant of the Cartesian plane is sigmoidal for any value of X_j, $j \neq i$. If $c_i = 1$, the graph of the function H_i^1 in the first quadrant is hyperbolic for any value of X_j, $j \neq i$ (although, in this paper, we generally call H_i^1 with $c_i \geq 1$ as sigmoid function). Moreover, when the value of c_i increases, the graph of $Y = H_i^1(X_i)$ gets steeper. If we add a term g_i to $H_i^1(X_i)$ then the graph of $Y = H_i^1(X_i)$ in the Cartesian plane is translated upwards by g_i units.

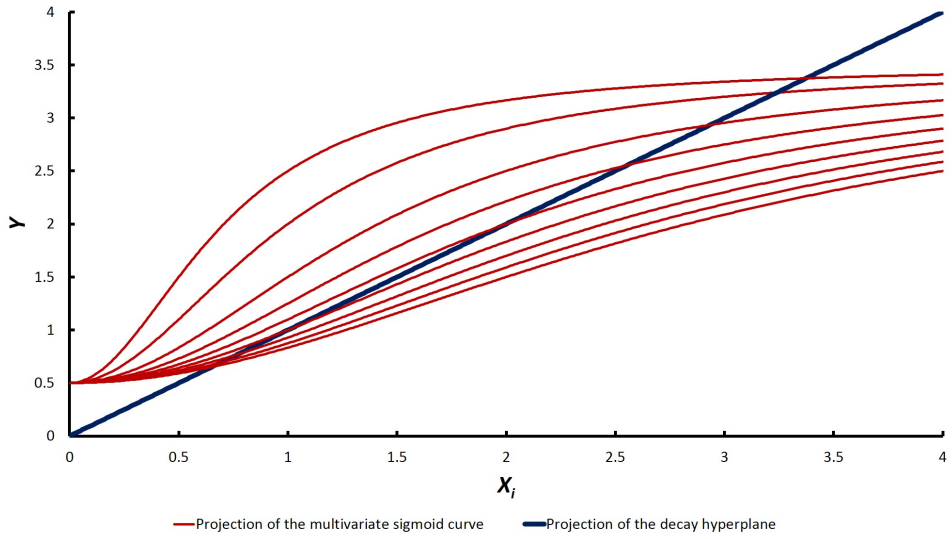

Figure 2: Projection of multivariate sigmoid function and decay hyperplane onto a Cartesian plane. We investigate the intersections of planar $Y = \rho_i X_i$ (line) and $Y = H_i^1(X_i) + g_i$ (sigmoid) with varying values of $\sum_{j \neq i} \gamma_{i,j} X_j^{c_{i,j}}$. Note that an intersection of the line and sigmoid curve is not necessarily a component of a steady state.

The geometric properties of the sigmoid function is essential in understanding the nature of the steady states. To find the steady states (equilibrium points), we need to solve the multivariate equation $F_i(X) = 0$ for all i (where F_i is given in the ODE system (1)). This implies that we need to determine the real solutions to

$$\frac{\beta_i X_i^{c_i}}{K_i + X_i^{c_i} + \sum_{j \neq i} \gamma_{i,j} X_j^{c_{i,j}}} + g_i = \rho_i X_i \text{ for all } i. \tag{5}$$

That is, we identify the intersections of the $n+1$-dimensional curve generated by the multivariate sigmoid function $H_i(X_1, X_2, ..., X_n)+g_i$ (left hand side of Equation (5)) and the $n+1$-dimensional decay hyperplane generated by $\rho_i X_i$ (right hand side of Equation (5)). For easier analysis, we rather examine the intersections of the univariate functions defined by $Y = H_i^1(X_i) + g_i$ and $Y = \rho_i X_i$ while varying the value of $\sum_{j \neq i} \gamma_{i,j} X_j^{c_{i,j}}$ in the denominator of the univariate sigmoid function H_i^1 (4) (see Figure (2) for illustration). In the univariate case, we can look at $Y = \rho_i X_i$

PeerJ PrePrints | http://dx.doi.org/10.7287/peerj.preprints.382v1 | CC-BY 4.0 Open Access | received: 8 May 2014, published: 8 May 2014

as a line in the Cartesian plane passing through the origin with slope equal to ρ_i.

Remark 1. It is always true that

$$\frac{\beta_i X_i^{c_i}}{K_i + X_i^{c_i}} \geq \frac{\beta_i X_i^{c_i}}{K_i + X_i^{c_i} + \sum_{j \neq i} \gamma_{i,j} X_j^{c_{i,j}}} \tag{6}$$

for any value of X_j for all j. In fact, if the value of $\sum_{j \neq i} \gamma_{i,j} X_j^{c_{i,j}}$ in the denominator of $H_i^1(X_i)$ increases, then the graph of the sigmoid curve $Y = H_i^1(X_i)$ shrinks (see Fig. (2)). Note that each X_j, $j \neq i$ is taken as a dynamic parameter but varying these parameters does not change the sigmoid shape of $Y = H_i^1(X_i)$.

One intuitive strategy for determining the stability of a steady state for a given set of parameter values is by doing component-wise stability analysis.

Definition 1. *Attracting component.* Let $X = (X_1, X_2, ..., X_i{}^*, ..., X_n)$, where X is not necessarily a steady state. Under the assumption that the value of $\sum_{j \neq i} \gamma_{i,j} X_j^{c_{i,j}}$ in the denominator of the univariate sigmoid function (4) is fixed, if X_i converges to X_i^* for all initial conditions near X_i^*, then we say that the i-th component X_i^* of X is attracting.

Property 1. *The steady state $X^* = (X_1{}^*, X_2{}^*, ..., X_n{}^*)$ of the CDM ODE system (1) is stable only if all its components are attracting. In other words, if at least one of the components of X^* is non-attracting, then X^* is unstable. The converse of this statement is not always true.*

Example 1. Consider the CDM ODE system (1) with $n = 3$, $\beta_i = 2$, $c_i = c_{i,j} = 3$, $K_i = 1$, $\gamma_{i,j} = 1$ and $\rho_i = 1$, for all $i, j = 1, 2, 3$. Let $g_1 = 0.1$, $g_2 = 0$ and $g_3 = 0$. We want to initially analyze the stability of one of the steady states, $(X_1{}^* = 0.10103, X_2{}^* = 1.001, X_3{}^* = 0)$, by employing Property (1). We test if a component is attracting or not by utilizing the geometric properties of the planar curves $Y = H_i^1(X_i) + g_i$ and $Y = \rho_i X_i$, $i = 1, 2, 3$.

The test is done by investigating the components one by one. Examine the intersection of $Y = H_1^1(X_1) + 1$ and $Y = X_1$ with $X_2 = 1.001$ and $X_3 = 0$ (Figure (3A)), then determine if $X_1{}^* = 0.10103$ is attracting using Figure (3D). We conclude that $X_1{}^* = 0.10103$ is an attracting component.

Now, test the attraction of $X_2{}^* = 1.001$ by looking at the intersection of $Y = H_2^1(X_2)$ and $Y = X_2$ with $X_1 = 0.10103$ and $X_3 = 0$ (Figure (3B)). Furthermore, test $X_3{}^* = 0$ by looking at the intersection of $Y = H_3^1(X_3)$ and $Y = X_3$ with $X_1 = 0.10103$ and $X_2 = 1.001$ (Figure (3C)). The tests reveal that $X_2{}^* = 1.001$ is non-attracting and $X_3 = 0$ is attracting.

PeerJ PrePrints | http://dx.doi.org/10.7287/peerj.preprints.382v1 | CC-BY 4.0 Open Access | received: 8 May 2014, published: 8 May 2014

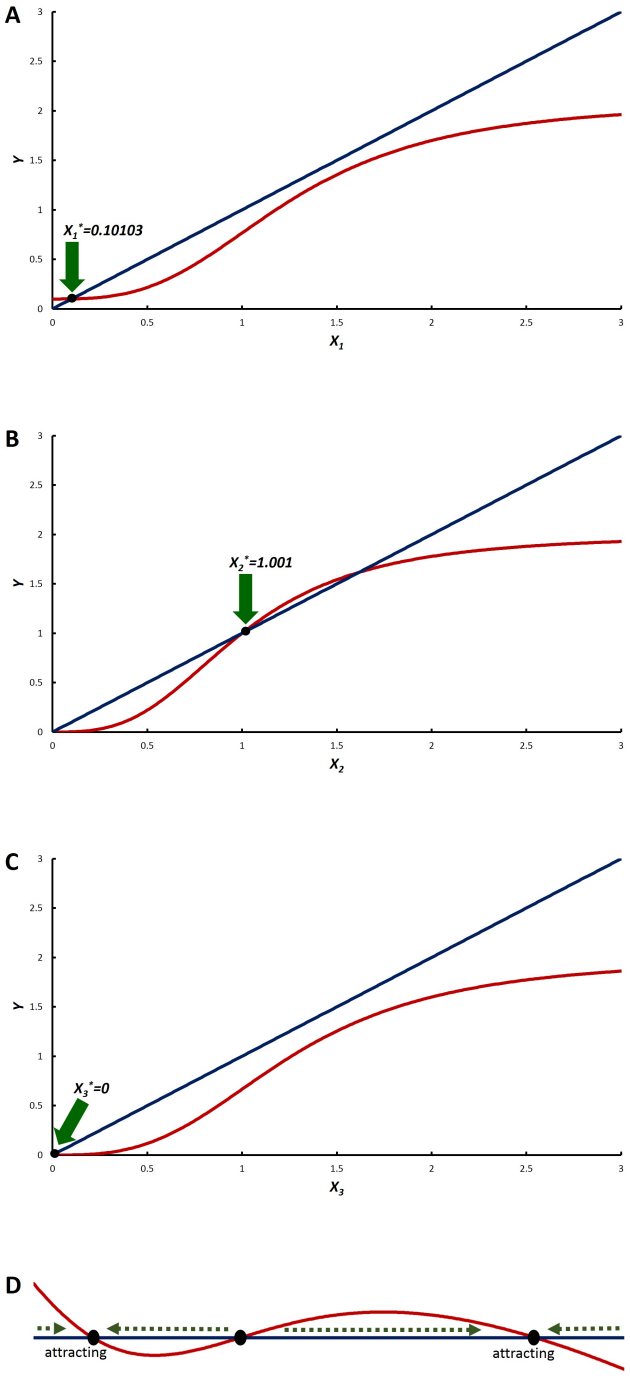

Figure 3: (**A**) Graphs of $Y = H_1^1(X_1) + 1$ and $Y = X_1$ with fixed $X_2 = 1.001$ and $X_3 = 0$ (refer to Example (1)). (**B**) Graphs of $Y = H_2^1(X_2)$ and $Y = X_2$ with fixed $X_1 = 0.10103$ and $X_3 = 0$. (**C**) Graphs of $Y = H_3^1(X_3)$ and $Y = X_3$ with fixed $X_1 = 0.10103$ and $X_2 = 1.001$. (**D**) The curves are rotated making the line $Y = \rho_i[X_i]$ as the horizontal axis. Positive gradient means non-attracting, negative gradient means attracting. If the gradient is zero, we look at the left and right neighboring gradients.

PeerJ PrePrints | http://dx.doi.org/10.7287/peerj.preprints.382v1 | CC-BY 4.0 Open Access | received: 8 May 2014, published: 8 May 2014

Therefore, the equilibrium point $(X_1{}^* = 0.10103, X_2{}^* = 1.001, X_3{}^* = 0)$ is unstable because of the presence of a non-attracting component $X_2{}^* = 1.001$.

Note that we can conclude that a steady state is unstable by using Property (1). However, we cannot immediately conclude if a steady state is stable by using component-wise stability analysis. There are exceptions where some unstable steady states have components that are all attracting (see Appendix A.1 for illustration). If the tests are inconclusive, we need to apply linearization technique using Jacobian matrix. The exceptions usually arise when there are oscillating solutions to the CDM ODE model (1).

2.2. Several types of equilibrium switching

Equilibrium switching can happen with and without changing parameter values (parameter regulation). To explain the scenarios of switching, suppose $n = 1$ (see Figure (4)). Figure (4A) shows noise-driven switching without parameter regulation. This noise-driven switching is possible in a system with multi-stable states [47, 48, 49, 41, 50, 51]. Figure (4B) is an example of switching by permanently changing a parameter value. On the other hand, Figure (4B) presents a strategy by temporarily varying the value of a parameter. This temporary change in parameter value drives the solution to the ODE model from one steady state's basin of attraction to another steady state's basin of attraction.

3. Results and Discussion

In this section, we present several mathematical properties of the CDM ODE model (1). Let the initial value $X_0 = (X_{1,0}, X_{2,0}, ..., X_{n,0})$ be non-negative real-valued. It follows that the solution to the ODE model (1) is always non-negative. Note that given non-negative state variables and parameters in the ODE system (1), if $g_i > 0$ then $\rho_i > 0$ for every i is a necessary and sufficient condition for the existence of a steady state.

Property 2. *Suppose $\rho_i > 0$. The value $\frac{g_i+\beta_i}{\rho_i}$ is an upper bound of, but will never be equal to, the attracting component X_i^*. The steady states of the CDM ODE system (1) lie in the hyperspace*

$$\left[\frac{g_1}{\rho_1}, \frac{g_1+\beta_1}{\rho_1}\right) \times \left[\frac{g_2}{\rho_2}, \frac{g_2+\beta_2}{\rho_2}\right) \times ... \times \left[\frac{g_n}{\rho_n}, \frac{g_n+\beta_n}{\rho_n}\right). \tag{7}$$

PeerJ PrePrints | http://dx.doi.org/10.7287/peerj.preprints.382v1 | CC-BY 4.0 Open Access | received: 8 May 2014, published: 8 May 2014

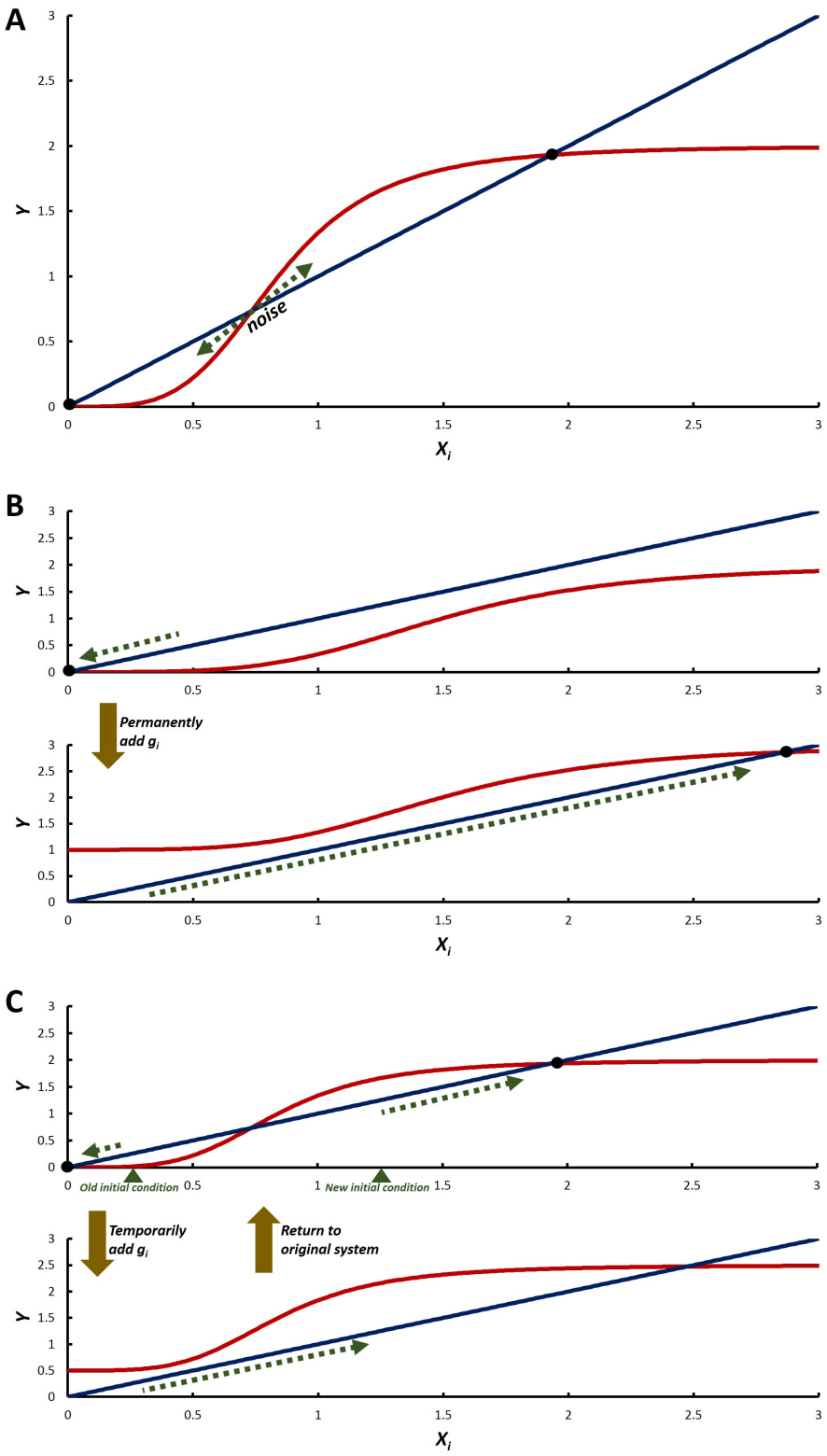

Figure 4: (**A**) Noise-driven equilibrium switching. (**B**) Switching by permanently changing a parameter value. (**C**) Switching by driving the solution to another basin of attraction through temporarily changing a parameter value.

PeerJ PrePrints | http://dx.doi.org/10.7287/peerj.preprints.382v1 | CC-BY 4.0 Open Access | received: 8 May 2014, published: 8 May 2014

Note that if both $g_i > 0$ and $\rho_i > 0$ then $X_i = g_i/\rho_i$ can only be an i-th component of a steady state of the ODE system (1) if $\beta_i = 0$. We can expand the size of the hyperspace (7) by increasing the value of g_i and β_i (maximal growth rate), and by decreasing the value of ρ_i (decay rate).

Property 3. *Suppose $\rho_i > 0$ for all i. Then each component of any state of the CDM ODE model (1) is always attracted by an attracting component. Note that this attraction does not necessarily mean convergence to equilibrium because the value of $\sum_{j\neq i} \gamma_{i,j} X_j^{c_{i,j}}$ in the denominator of the sigmoid function (4) can vary.*

The convergence to a steady state, where every X_i converges to an attracting component $X_i{}^*$ for the given initial condition, is common to CDM ODE models with symmetric interaction matrix (e.g., $\gamma_{i,j} = \gamma$ for all i, j, γ is a constant). However, an attracting component can either be a coordinate of an equilibrium point or an attractor that induces sustained oscillations. These sustained oscillations are due to the varying value of $\sum_{j\neq i} \gamma_{i,j}[X_j]^{c_{i,j}}$ in the denominator of the sigmoid function that causes continuous change in the intersections of $Y = H_i^1(X_i) + g_i$ and $Y = \rho_i[X_i]$.

Property 4. *Suppose sustained oscillations exist. The value of $\frac{g_i+\beta_i}{\rho_i}$ is an upper bound of the sustained oscillating solution to X_i. The sustained oscillations of the CDM ODE system (1) is contained in the hyperspace (7).*

Example 2. One example of such oscillating system is a repressilator (a type of synthetic biological oscillator [52, 53, 54, 55, 56, 57]) of the form

$$\begin{aligned}
\frac{dX_1}{dt} &= \frac{X_1^2}{1 + X_1^2 + X_2^2 + 0.1X_3^2} - 0.1X_1 + 0.1 \\
\frac{dX_2}{dt} &= \frac{X_2^2}{1 + 0.1X_1^2 + X_2^2 + X_3^2} - 0.1X_2 + 0.1 \\
\frac{dX_3}{dt} &= \frac{X_3^2}{1 + X_1^2 + 0.1X_2^2 + X_3^2} - 0.1X_3 + 0.1.
\end{aligned} \tag{8}$$

Notice that the interaction among components in this example is asymmetric where one direction of inhibition is stronger than the reverse direction (Appendix A.1). According to various mathematical propositions from previous studies, such as the Thomas' rules, positive circuits (e.g., two mutually inhibiting components with symmetric reciprocal repression) induce multi-stability, and negative circuit (e.g., asymmetric inhibition among three components that forms a repressilator) induce oscillations [58, 59, 60, 61].

PeerJ PrePrints | http://dx.doi.org/10.7287/peerj.preprints.382v1 | CC-BY 4.0 Open Access | received: 8 May 2014, published: 8 May 2014

Now, suppose c_i and $c_{i,j}$ are integers for all i and j. The corresponding polynomial equation to

$$F_i(X) = \frac{\beta_i X_i^{c_i}}{K_i + X_i^{c_i} + \sum_{j \neq i} \gamma_{i,j} X_j^{c_{i,j}}} - \rho_i X_i + g_i = 0 \tag{9}$$

is

$$P_i(X) = \beta_i X_i^{c_i} + (g_i - \rho_i X_i) \left(K_i + X_i^{c_i} + \sum_{j \neq i} \gamma_{i,j} X_j^{c_{i,j}} \right) = 0 \text{ for all } i. \tag{10}$$

Property 5. *Under the assumption that that there is only a finite number of steady states, the number of steady states of the CDM ODE model (1) (where c_i and $c_{i,j}$ are integers) is at most*

$$\prod_{i=1}^{n} max\{c_i + 1, c_{i,j} + 1 \text{ for all } j \neq i\}. \tag{11}$$

The proof of Property (5) is by Bézout Theorem [62] applied to the system of polynomial equations (10). Bézout Theorem does not give the exact number of steady states but only the upper bound. From Property (5), the maximum number of steady states is dependent on the value of c_i and $c_{i,j}$ as well as on n (dimension of our state space). Note that the size of the basin of attraction of a steady state depends on the number of existing steady states and on the size of the hyperspace (7). The hyperspace (7) is fixed for a given set of parameter values, and the basin of attraction of each existing steady state is distributed in this hyperspace. If there are multiple stable steady states then there are multiple basins of attraction that share the region of the hyperspace.

We classify the stable steady states based on its dominant component. The following definition of terms are used to classify the steady states.

Definition 2. *Classification of steady states.* A component is switched-off (inactive or extinct) if its value is zero, and switched-on otherwise. A switched-on X_i dominates X_j if $X_j/X_i < \epsilon \leq 1$, where $\epsilon > 0$ is an acceptable tolerance constant.

- 1-node dominance or premier state refers to the case where a stable steady state has only one dominant component;
- p-node co-dominance refers to the case where a stable steady state has p dominant components such that the dominant components have equal values; and

PeerJ PrePrints | http://dx.doi.org/10.7287/peerj.preprints.382v1 | CC-BY 4.0 Open Access | received: 8 May 2014, published: 8 May 2014

- n-node co-dominance or priming state refers to the case where all components of a stable steady state have equal positive values.

Suppose we want the i-th component of a state to be the dominant, then we say that X is a desired steady state if the component X_i^* of X is dominant.

Example 3. Consider the CDM ODE model (1) with $n = 2$, $c_i = c_{i,j} = 1$ and $g_i = 0$, $i, j = 1, 2$. If the number of steady states is finite, then we expect that the maximum number of possible steady states is 4. The possible steady states are

- Zero state (all components are switched-off): $(0, 0)$. This is stable when $\beta_i < \rho_i K_i$, for all $i = 1, 2$.
- One component is switched-on: $\left(0, \frac{\beta_2 - \rho_2 K_2}{\rho_2}\right)$. This is a steady state if $\beta_2 > \rho_2 K_2$, and stable (premier state) if $\beta_1 < \rho_1 \left(K_1 + \gamma_{1,2} \frac{\beta_2 - \rho_2 K_2}{\rho_2}\right)$.
- One component is switched-on: $\left(\frac{\beta_1 - \rho_1 K_1}{\rho_1}, 0\right)$. This is a steady state if $\beta_1 > \rho_1 K_1$, and stable (premier state) if $\beta_2 < \rho_2 \left(K_2 + \gamma_{2,1} \frac{\beta_1 - \rho_1 K_1}{\rho_1}\right)$.
- All components are switched-on:
  $\left(\frac{\beta_1 - \rho_1\left(K_1 + \gamma_{1,2}\left(\frac{\beta_2}{\rho_2} - K_2\right)\right)}{\rho_1(1 - \gamma_{1,2}\gamma_{2,1})}, \frac{\beta_2 - \rho_2\left(K_2 + \gamma_{2,1}\left(\frac{\beta_1}{\rho_1} - K_1\right)\right)}{\rho_2(1 - \gamma_{2,1}\gamma_{1,2})}\right)$.
  This state is likely to be stable if it exists. This state satisfies
  $\left(\frac{\beta_1 - \rho_1\left(K_1 + \gamma_{1,2} X_2^*\right)}{\rho_1}, \frac{\beta_2 - \rho_2\left(K_2 + \gamma_{2,1} X_1^*\right)}{\rho_2}\right) = (X_1^*, X_2^*)$.

There are cases where the polynomial system (10) has infinitely many complex-valued solutions, hence, Property (5) does not apply. Infinitely many steady states could arise if all equations in the polynomial system (10) have a common factor of degree greater than zero.

Property 6. *Suppose $c_i = c_{i,j} = 1$, $K_i = K > 0$, $\gamma_{i,j} = 1$, $g_i = 0$, $\beta_i = \beta > 0$ and $\rho_i = \rho > 0$ where $\beta > \rho K$ for all i and j (K, β and ρ are constants). Then the polynomial system associated to the CDM ODE model (1) has a non-constant common factor. Any CDM ODE model that can be converted to this type of polynomial system has infinitely many steady states.*

Example 4. An example of a CDM ODE model having infinitely many equilibrium points is

PeerJ PrePrints | http://dx.doi.org/10.7287/peerj.preprints.382v1 | CC-BY 4.0 Open Access | received: 8 May 2014, published: 8 May 2014

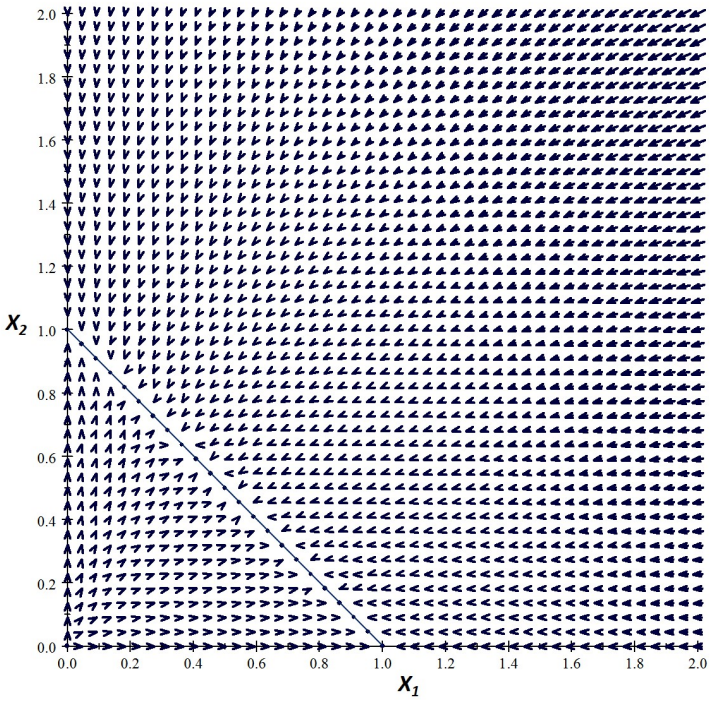

Figure 5: A phase plane showing an attracting line. Parameter values are $n = 2$, $c_1 = c_2 = c_{1,2} = c_{2,1} = 1$, $K_1 = K_2 = 1$, $\gamma_{1,2} = \gamma_{2,1} = 1$, $g_1 = g_2 = 0$, $\beta_1 = 2$, $\beta_2 = 1$, $\rho_1 = 1$ and $\rho_2 = 1/2$.

of the form

$$\frac{dX_i}{dt} = \frac{AX_i}{K + X_i + \sum_{j \neq i} X_j} - X_i, \ i = 1, 2, ..., m \tag{12}$$

$$\frac{dX_k}{dt} = \frac{X_k}{K + X_k + \sum_{j \neq k} X_j} - \frac{X_k}{A}, \ k = m+1, m+2, ..., n$$

where $A > K \geq 1$ is a constant (see Figure (5) for illustration). The polynomial system (10) of this CDM ODE model is similar to the polynomial system of the CDM ODE model described in Property (7) with $\beta = A$ and $\rho = 1$.

Property 7. *Suppose $c_i = c_{i,j} = 1$, $K_i = K > 0$, $\gamma_{i,j} = 1$, $g_i = 0$, $\beta_i = \beta > 0$ and $\rho_i = \rho > 0$ for all i and j (K, β and ρ are constants). If $\beta > \rho K$ then the steady states of the ODE system (1) are the zero state and the non-isolated points lying on the hyperplane with equation*

$$\sum_{j=1}^{n} X_j = \frac{\beta}{\rho} - K, \ X_j \geq 0 \text{ for all } j. \tag{13}$$

PeerJ PrePrints | http://dx.doi.org/10.7287/peerj.preprints.382v1 | CC-BY 4.0 Open Access | received: 8 May 2014, published: 8 May 2014

In addition, the zero state is an unstable equilibrium point while the hyperplane (13) is an attractor.

The convergence to the zero state $(0, 0, ..., 0)$ implies that all components eventually switch-off. Note that the CDM ODE model (1) has a steady state with i-th component $X_i^* = 0$ if and only if $g_i = 0$. The zero state of the ODE system (1) can only be a steady state if and only if $g_i = 0$ for all i.

In general, suppose $g_i = 0$ for all i, then the zero state is the only equilibrium point of the ODE model (1) if the univariate curve $Y = H_i^1(X_i)$ lies below the decay line $Y = \rho_i X_i$ (i.e., $H_i^1(X_i) < \rho_i X_i$, for all $X_i > 0$) for every $i = 1, 2, ..., n$. This phenomenon indicates that the exponential decay of each component is faster than stimulation, thus, we expect that all components will eventually be switched-off given any initial condition.

Property 8. *If $c_i > 1$, $g_i = 0$ and*

$$\rho_i({K_i}^{1/c_i}) \geq \beta_i \tag{14}$$

for all i, then the CDM ODE system (1) has only one equilibrium point which is the zero state because we are sure that the univariate curve $Y = H_i^1(X_i)$ lies below the decay line $Y = \rho_i X_i$.

In addition, if $c_i = 1$, $g_i = 0$ and $\beta_i/K_i \leq \rho_i$ for all i, then the ODE system (1) has the zero state as the sole equilibrium point.

The following property present cases where the solution to the ODE system (1) converges to the zero state (depending on the initial condition):

Property 9. *In the CDM ODE system (1), suppose $c_i = 1$ and $g_i = 0$ for all i. Then the zero state is a stable equilibrium point when $\rho_i > \beta_i/K_i$ for all i, or an unstable equilibrium point when $\rho_i < \beta_i/K_i$ for at least one i. If $\rho_i = \beta_i/K_i$ for at least one i, then we have an attractor only when X_i is restricted to be non-negative and $\rho_j \geq \beta_j/K_j$ for every $j \neq i$.*

In addition, suppose $c_i > 1$, $\rho_i > 0$ and $g_i = 0$ for all i. Then the zero state is a stable equilibrium point of the ODE system (1).

Remark 2. Suppose $c_i > 1$, $\rho_i > 0$ and $g_i = 0$. Then $X_i^* = 0$ is always an attracting component.

Remark (2) is important because this suggests that if the i-th component is switched-off then it can never be switched-on again, unless we effectively perturb the system by introducing

PeerJ PrePrints | http://dx.doi.org/10.7287/peerj.preprints.382v1 | CC-BY 4.0 Open Access | received: 8 May 2014, published: 8 May 2014

an additive external stimulus (s_i) or some stochastic noise [63, 49, 48, 41]. In some cases where a zero attracting component is unwanted, a modified CDM ODE model can be used, such as

$$\frac{dX_i}{dt} = \frac{\beta_i \exp(c_i(X_i - \delta_i))}{K_i + \exp(c_i(X_i - \delta_i)) + \sum_{j \neq i} \gamma_{i,j} \exp(c_{i,j} X_j)} + g_i - \rho_i X_i, \quad \text{for } i = 1, 2, ..., n. \tag{15}$$

The parameter δ_i shifts the sigmoid kinetics of the i-th component to higher values of X_i. In cellular differentiation [64, 65], the zero state has trivial biological importance because it does not represent any phenotype.

3.1. Equilibrium switching by parameter regulation

Property 10. *Varying the values of some parameters of the CDM ODE model (1) can enable equilibrium switching from one stable steady state to another.*

We can mathematically manipulate the parameter values to ensure that the initial condition is in the basin of attraction of the desired steady state. We can do this by decreasing the size of the basin of attraction of an undesired steady state as well as increasing the size of the basin of attraction of the desired steady state. For example, we can force the i-th component of a state to eventually dominate other components by increasing the maximal growth rate $\beta_i + g_i$ [66, 67, 68, 69, 70] or by decreasing the decay rate ρ_i (Figure (6A-C)) [71, 72, 73, 74].

We assume that changes in external stimuli are represented in the variations of the parameter g_i. The parameter g_i is assumed as a constant production term that alters the maximum value of the multivariate sigmoid function. If we increase the value of g_i then the value of the attracting component X_i^* where $Y = H_i^1(X_i) + g_i$ and $Y = \rho_i(X_i)$ intersect also increases. In fact, we can force such enhanced value of X_i^* to be the only intersection even if the value of $\sum_{j \neq i} \gamma_{i,j} X_j^{c_{i,j}}$ increases (see Figure (7A) for illustration).

The component X_i inhibits X_j, hence, if we increase the value of X_i^* by adding g_i then the value of X_j^*, $j \neq i$ where $Y = H_j^1(X_j) + g_j$ and $Y = \rho_j(X_j)$ intersect decreases. We can actually force such decreased value of X_j^* to be the only intersection by amplifying g_i up to a sufficient level (note that if $g_j = 0$, then it is possible to make the switched-off $X_j^* = 0$ the only attracting component). Therefore, by sufficiently changing the value of g_i we can have a sole stable steady state where the i-th component dominates the others ($X_i^* > X_j^*$, $j \neq i$). For any initial condition, the solution to the CDM ODE model (1) converges to this sole steady state.

PeerJ PrePrints | http://dx.doi.org/10.7287/peerj.preprints.382v1 | CC-BY 4.0 Open Access | received: 8 May 2014, published: 8 May 2014

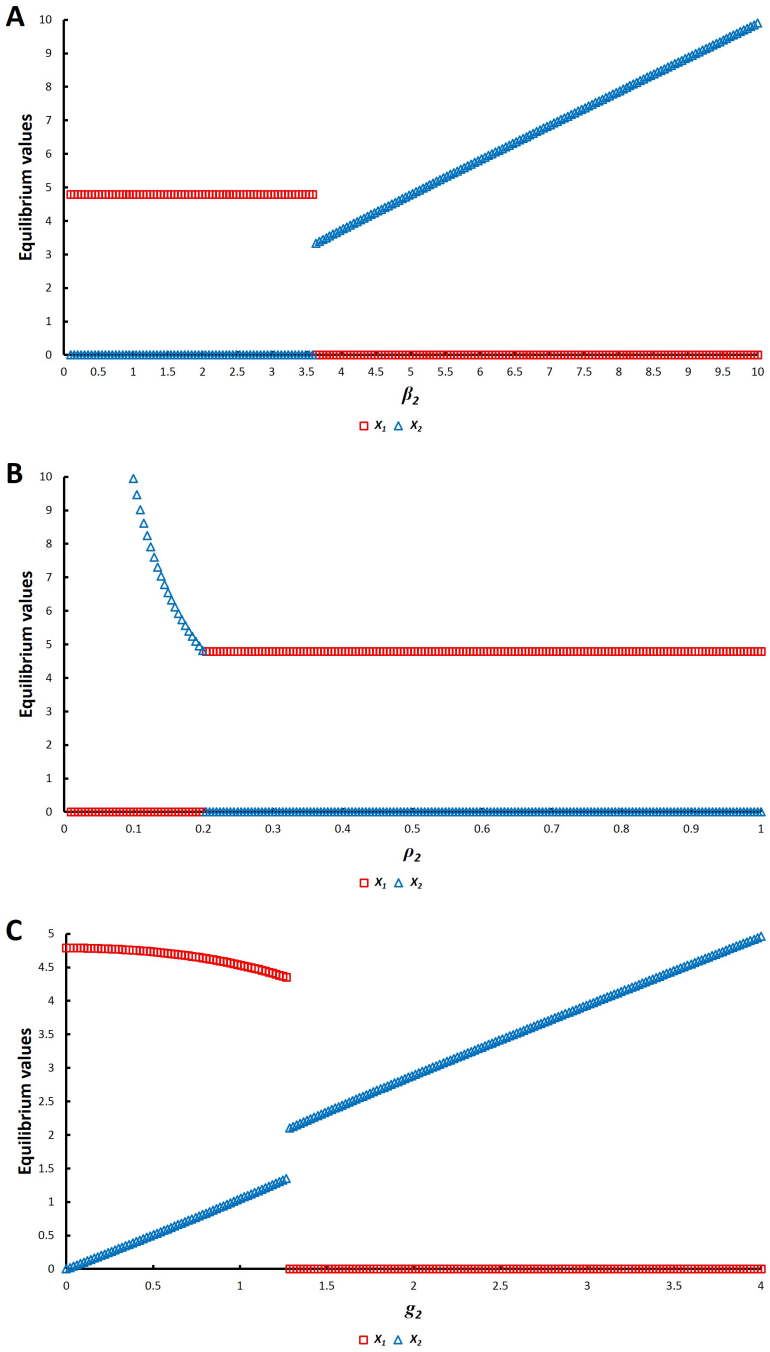

Figure 6: Let $n = 2$, $c_1 = c_2 = c_{1,2} = c_{2,1} = 1$, $\beta_1 = 1$, $K_1 = K_2 = 1$, $\gamma_{1,2} = \gamma_{2,1} = 1$, $\rho_1 = 0.2$ and $g_1 = 0$. (**A**) Varying the value of β_2 can switch equilibrium states. Initial values are set to $X_{1,0} = 1$ and $X_{2,0} = 1$, and parameter values are $\rho_2 = 1$ and $g_2 = 0$. (**B**) Varying the value of ρ_2 can switch equilibrium states. Initial values are set to $X_{1,0} = 1$ and $X_{2,0} = 1$, and parameter values are $\beta_2 = 1$ and $g_2 = 0$. (**C**) Varying the value of g_2 can switch equilibrium states even though the initial condition of X_2 is switched-off. Initial values are set to $X_{1,0} = 1$ and $X_{2,0} = 0$, and parameter values are $\beta_2 = 1$ and $\rho_2 = 1$.

PeerJ PrePrints | http://dx.doi.org/10.7287/peerj.preprints.382v1 | CC-BY 4.0 Open Access | received: 8 May 2014, published: 8 May 2014

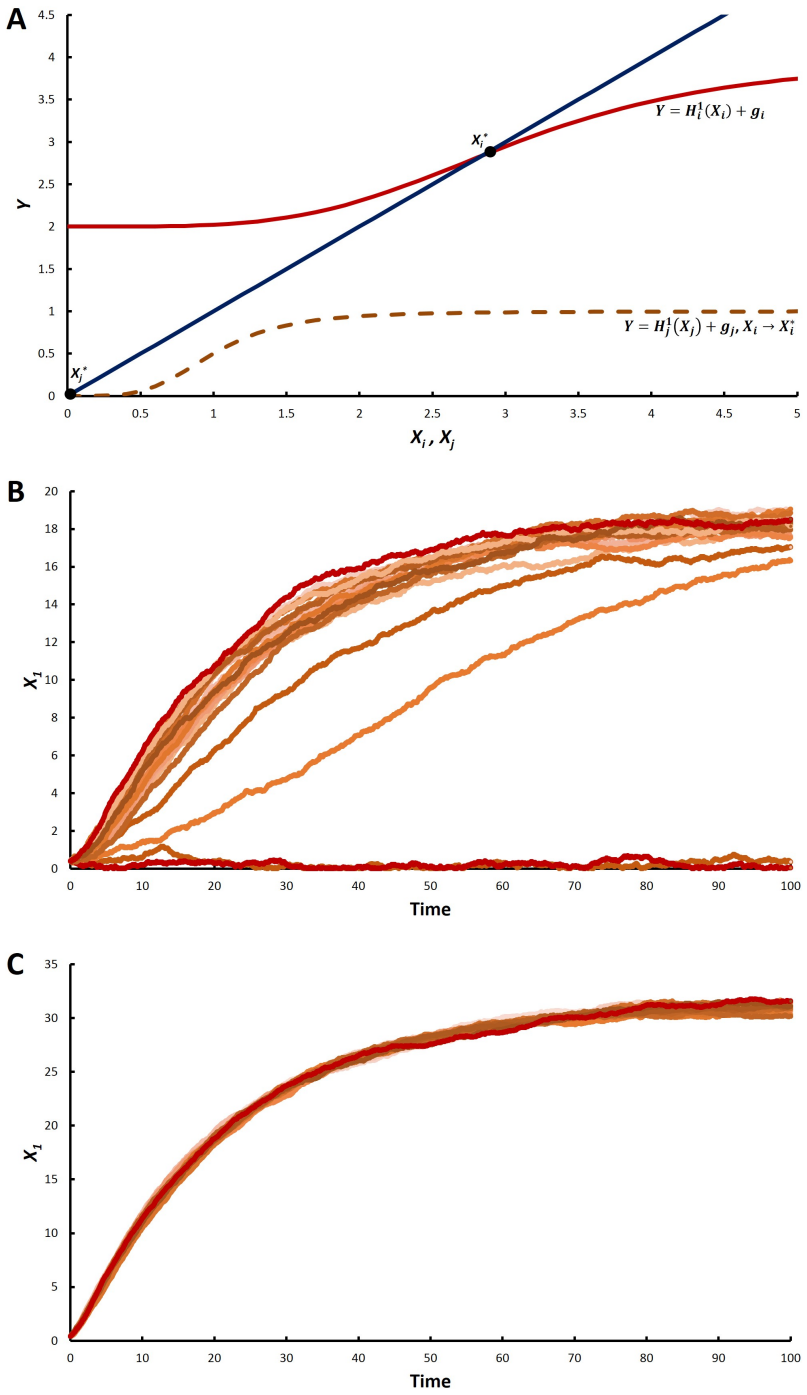

Figure 7: (**A**) Increasing the value of g_i can steer X_i to converge to high-valued X_i^*, and X_j to converge to low-valued X_j^*. (**B**) Let us consider the ODE model in Example (16) but set $g_1 = dW$ where dW is a Gaussian white noise (see [41]). Stochastic noise can drive sample paths to different steady states of the CDM ODE model. Out of the 20 simulation runs, 2 of the sample paths tend to the lower-valued attracting component. Initial condition is $(0.4, 0.5)$, only the sample paths of X_1 are shown in the figure. (**C**) Setting $g_1 = 0.5 + dW$, all sample paths out of the 20 simulation runs tend to the sole steady state of the CDM ODE model. Initial condition is $(0.4, 0.5)$, only the sample paths of X_1 are shown in the figure.

PeerJ PrePrints | http://dx.doi.org/10.7287/peerj.preprints.382v1 | CC-BY 4.0 Open Access | received: 8 May 2014, published: 8 May 2014

The perpetual addition of sufficient amount of external stimulus, represented by constant g_i, can shutdown the multi-stability of the system such that only one stable steady state remains. Thus, this strategy increases the robustness of the solution to the CDM ODE model against stochastic noise that induces equilibrium switching. Figure (7B) shows that stochastic noise can drive sample paths (solutions to stochastic differential equations) to different stable steady states of the CDM ODE model. However, adding a constant supply of external stimulus can minimize this noise-driven switching as illustrated in Figure (7C).

Example 5. Consider the CDM ODE model (1) of the form:

$$\begin{aligned} \frac{dX_1}{dt} &= \frac{X_1^2}{1 + X_1^2 + \frac{1}{8}X_2^2} - \frac{1}{21}X_1 \\ \frac{dX_2}{dt} &= \frac{X_2^2}{1 + \frac{1}{8}X_1^2 + X_2^2} - \frac{1}{21}X_2. \end{aligned} \tag{16}$$

This system has 9 steady states which is equal to the Bézout upper bound (Property (5)). There are only 4 stable steady states out of the 9. The four stable steady states represent a 2-node dominance, two premier states (1-node dominance) and a zero state (see Appendix B for the numerical results).

Now, suppose we introduce $g_1 = 0.5$. Introducing $g_1 = 0.5$ forces X_1 to converge to the high-valued attracting component X_1^*, and forces

$$\frac{X_2^2}{1 + \frac{1}{8}X_1^{*2} + X_2^2} < \frac{1}{21}X_2 \tag{17}$$

for all values of X_2. Hence, there will be exactly one steady state. This steady state is stable and represents a premier state where X_1^* is dominant and X_2^* is switched-off.

The parameters K_i, c_i, $c_{i,j}$ and $\gamma_{i,j}$ do not affect the upper bound of the hyperspace (7). However, increasing K_j for all $j \neq i$ can force each X_j to converge to the lower-valued attracting component (or even be switched-off when $g_j = 0$). This increases the chance of X_i to converge to $X_i^* > X_j^*$ for all $j \neq i$. Furthermore, increasing the value of c_i or $c_{i,j}$ can result in an increased number of steady states (by Property (5)). Varying the values of these exponents can prompt steady state switching (Figure (8)) and can also result in oscillations (see Appendix A.2).

There are cases where the interaction coefficients ($\gamma_{i,j}$) act as controls to induce steady state switching. Increasing the inhibition strength of one component can affect its dominance over the other components. For example, recall the steady state in Example (3) for $n = 2$ with

PeerJ PrePrints | http://dx.doi.org/10.7287/peerj.preprints.382v1 | CC-BY 4.0 Open Access | received: 8 May 2014, published: 8 May 2014

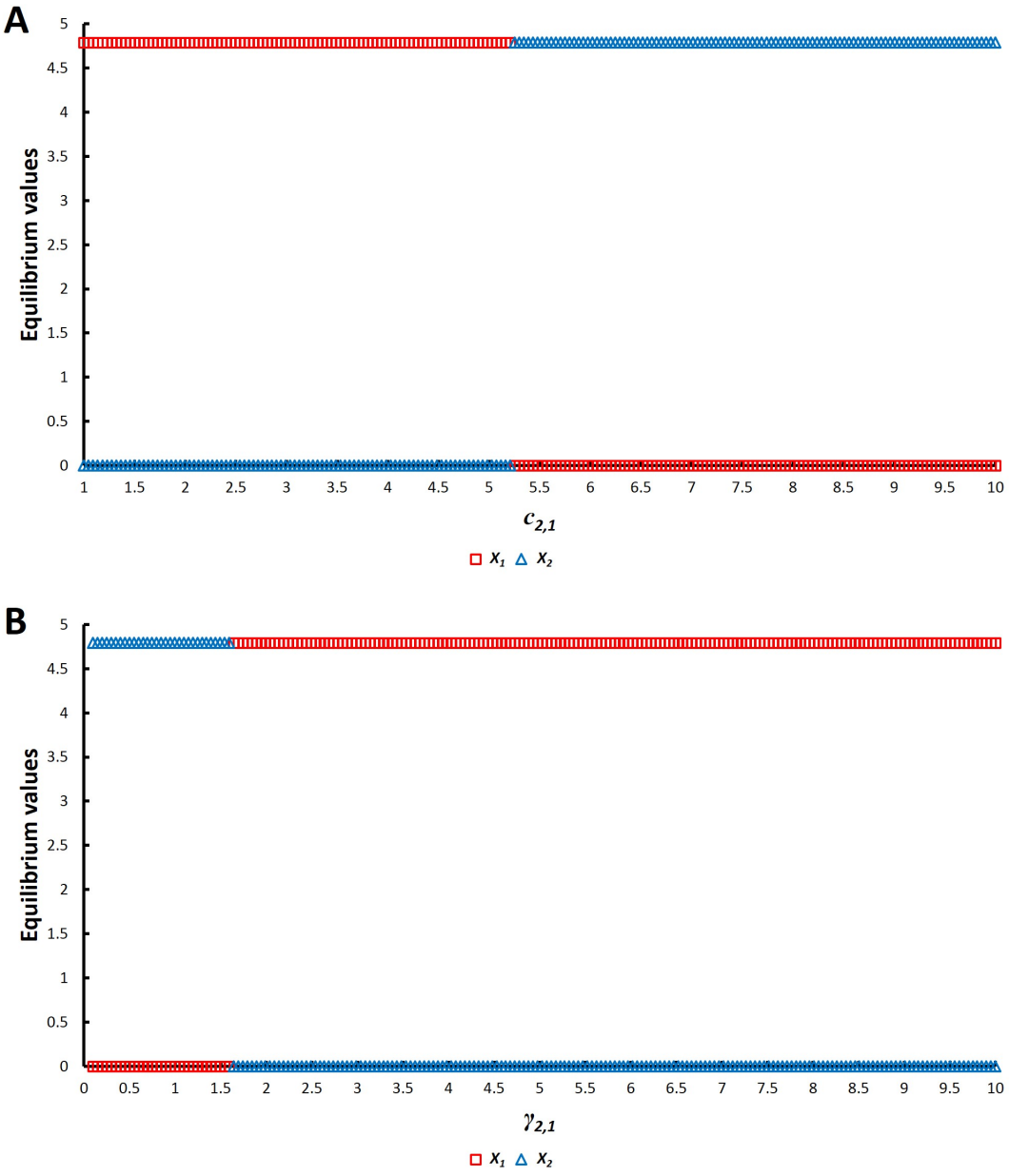

Figure 8: Increasing the inhibition exponent $c_{2,1}$ and interaction coefficient $\gamma_{2,1}$ can drive equilibrium switching. Let $n = 2$, $X_0 = (1, 1.2)$, $c_1 = c_2 = c_{1,2} = 2$, $\beta_1 = \beta_2 = 1$, $K_1 = K_2 = 1$, $\gamma_{1,2} = 1$, $\rho_1 = \rho_2 = 0.2$ and $g_1 = g_2 = 0$. (**A**) Varying the value of $c_{2,1}$. (**B**) Varying the value of $\gamma_{2,1}$.

PeerJ PrePrints | http://dx.doi.org/10.7287/peerj.preprints.382v1 | CC-BY 4.0 Open Access | received: 8 May 2014, published: 8 May 2014

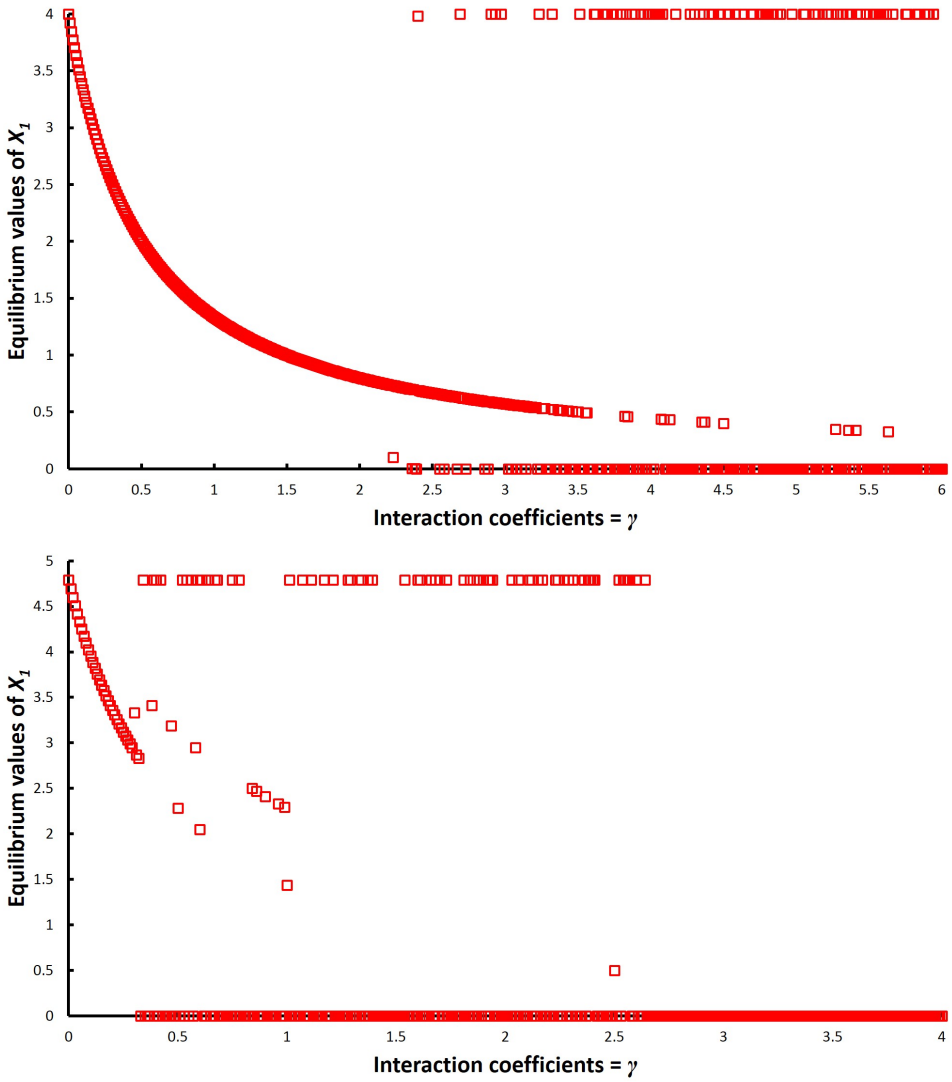

Figure 9: Varying the interaction coefficients can prompt steady state switching. Suppose $n = 3$, $X_0 = (0.5, 0.5, 0.5)$, $g_i = 0$, $\gamma_{i,j} = \gamma$, $\beta_i = 1$, $\rho_i = 0.2$ and $K_i = 1$, for all i, j. Only the equilibrium values of X_1 are shown. (**A**) Let $c_i = c_{i,j} = 1$ for all i, j. (**B**) Let $c_i = c_{i,j} = 2$ for all i, j.

PeerJ PrePrints | http://dx.doi.org/10.7287/peerj.preprints.382v1 | CC-BY 4.0 Open Access | received: 8 May 2014, published: 8 May 2014

$c_i = c_{i,j} = 1$ and $g_i = 0$, $i, j = 1, 2$,

$$\left(\frac{\beta_1 - \rho_1 \left(K_1 + \gamma_{1,2} X_2^* \right)}{\rho_1}, \frac{\beta_2 - \rho_2 \left(K_2 + \gamma_{2,1} X_1^* \right)}{\rho_2} \right). \tag{18}$$

Notice that as we enhance the inhibition of X_1 by X_2, represented by $\gamma_{1,2}$, it can drive $\beta_1 < \rho_1 \left(K_1 + \gamma_{1,2} X_2^* \right)$ that switches-off X_1^*. This drives X_2 to eventually dominate X_1.

The diagrams in Figure (9) present additional illustrations of steady state switching by varying the value of the interaction coefficients. However, regulating the interaction among components is not always as straightforward as regulating the values of β_i, g_i and ρ_i in steering the system toward the desired steady state. Having an asymmetric interaction matrix can generate oscillating behavior, such as the repressilator (Appendix A.1).

Oscillations can lead to state switching for some period of time. If the solution attains a desired temporal condition, we can dampen the oscillating behavior (e.g., by parameter regulation from asymmetric to symmetric $[\gamma_{i,j}]$) to have stability where the desired outcome is maintained (Appendix A.3). This is a strategy where oscillations and stability both assist in driving a solution towards the desired equilibrium [75]. To avoid volatile effect of randomness, the oscillation-driven switching can be an alternative to the the noise-driven switching but only when oscillation is structurally feasible.

4. Conclusions

We are able to show the qualitative dynamics of the CDM by investigating the mathematical properties of its associated system of ordinary differential equations (ODE) with nonlinear kinetics. The CDM can predict multi-stability that may give rise to co-existence or to domination by some components. Regulating the maximal growth rate (which is possibly influenced by an external stimulus), decay rate and interaction among components can affect the nature of the steady states. Parameter regulation is a possible deterministic strategy for controlling the dominance of a component towards the desired steady state. The introduction of an external stimulus can result in a system with a sole attractor, which can control the effect of moderate stochastic noise.

In some cases, CDM can also represent synthetic biological oscillators. Combining the effect of oscillation and stability can be a potential strategy for attaining the desired outcome. Asymmetric strength of inhibition among components can result in sustained oscillations, but this is

PeerJ PrePrints | http://dx.doi.org/10.7287/peerj.preprints.382v1 | CC-BY 4.0 Open Access | received: 8 May 2014, published: 8 May 2014

not true for all asymmetric systems. Our study can be extended to search for general conditions that generate oscillatory behavior.

If we want to reactivate a switched-off component then one strategy is to add an external stimulus that enhances the basal growth. However, it is sometimes impractical or infeasible to continuously add such a constant amount of inducement. Consequently, we may rather consider an external stimulus that varies through time. If there are multiple stable steady states, introducing a varying amount of stimulus can affect the long-term outcome of the CDM dynamics through equilibrium switching. If deterministic parameter regulation is not perpetually possible, combining deterministic and stochastic techniques could be done, such as by supplementing the effect of external stimulus with stochastic fluctuations.

Supplementary Material

For the proofs of the mathematical properties and additional illustrations, see the supporting text in the Supplementary Material. Send an e-mail to the author to obtain the Supplementary Material.

References

[1] B. Barzel, A.-L. Barabasi, Universality in network dynamics, Nature Phys. 9 (2013) 673–681. doi:10.1038/nphys2741.

[2] Y.-Y. Liu, J.-J. Slotine, A.-L. Barabasi, Observability of complex systems, PNAS 110 (7) (2013) 2460–2465. doi:10.1073/pnas.1215508110.

[3] F. S. Neves, M. Timme, Computation by switching in complex networks of states, Phys. Rev. Lett. 109 (2012) 018701. doi:10.1103/PhysRevLett.109.018701.

[4] H. Neumeister, K. W. Whitaker, H. A. Hofmann, T. Preuss, Social and ecological regulation of a decision-making circuit, J. Neurophysiol. 104 (6) (2010) 3180–3188. doi:10.1152/jn.00574.2010.

[5] S. Boccaletti, V. Latora, Y. Moreno, M. Chavez, D.-U. Hwang, Complex networks: Structure and dynamics, Phys. Rep. 424 (2006) 175–308. doi:10.1016/j.physrep.2005.10.009.

PeerJ PrePrints | http://dx.doi.org/10.7287/peerj.preprints.382v1 | CC-BY 4.0 Open Access | received: 8 May 2014, published: 8 May 2014

[6] J. Panovska-Griffiths, K. M. Page, J. Briscoe, A gene regulatory motif that generates oscillatory or multiway switch outputs, J. R. Soc. Interface 10 (79) (2012) 20120826. doi:10.1098/rsif.2012.0826.

[7] B. L. Baumgartner, M. R. Bennett, M. Ferry, T. L. Johnson, L. S. Tsimring, J. Hasty, Antagonistic gene transcripts regulate adaptation to new growth environments, PNAS 108 (52) (2011) 21087–21092. doi:10.1073/pnas.1111408109.

[8] E. H. Davidson, Emerging properties of animal gene regulatory networks, Nature 468 (2010) 911–920. doi:10.1038/nature09645.

[9] J. Macia, S. Widder, R. Sole, Why are cellular switches boolean? general conditions for multistable genetic circuits, J. Theor. Biol. 261 (2009) 126–135. doi:10.1016/j.jtbi.2009.07.019.

[10] R. Guantes, J. F. Poyatos, Multistable decision switches for flexible control of epigenetic differentiation, PLoS Comput. Biol. 4 (11) (2008) e1000235. doi:10.1371/journal.pcbi.1000235.

[11] V. Chickarmane, C. Troein, U. A. Nuber, H. M. Sauro, C. Peterson, Transcriptional dynamics of the embryonic stem cell switch, PLoS Comput. Biol. 2 (9) (2006) e123. doi:10.1371/journal.pcbi.0020123.

[12] E. Kaarlejarvi, J. Olofsson, Concurrent biotic interactions influence plant performance at their altitudinal distribution margins, Oikos (2014) (online)doi:10.1111/oik.01261.

[13] G. Huguet, J. Rinzel, J. Hupe, Noise and adaptation in multistable perception: noise drives when to switch, adaptation determines percept choice, J. Vis. 14 (3) (2014) 1–24. doi:10.1167/14.3.19.

[14] A. Mougi, M. Kondoh, Diversity of interaction types and ecological community stability, Science 337 (2012) 349–351. doi:10.1126/science.1220529.

[15] S. B. Jeswiet, S. S. Lee-Jenkins, J.-G. J. Godin, Concurrent effects of sperm competition and female quality on male mate choice in the trinidadian guppy (*Poecilia reticulata*), Behav. Ecol. 23 (1) (2011) 195–200. doi:10.1093/beheco/arr175.

PeerJ PrePrints | http://dx.doi.org/10.7287/peerj.preprints.382v1 | CC-BY 4.0 Open Access | received: 8 May 2014, published: 8 May 2014

[16] N. Ganguly, A. Deutsch, A. Mukherjee (Eds.), Dynamics On and Of Complex Networks: Applications to Biology, Computer Science, and the Social Sciences, Birkhauser, Boston, 2009.

[17] O. Cinquin, J. Demongeot, High-dimensional switches and the modelling of cellular differentiation, J. Theor. Biol. 233 (2005) 391–411. doi:10.1016/j.jtbi.2004.10.027.

[18] A. N. Pisarchik, U. Feudel, Control of multistability, Phys. Rep. (2014) (online)doi:10.1016/j.physrep.2014.02.007.

[19] B. Luna, E. Galan-Vasquez, E. Ugalde, A. Martinez-Antonio, Structural comparison of biological networks based on dominant vertices, Mol. Biosyst. 9 (2013) 1765–1773. doi:10.1039/c3mb70077a.

[20] N. J. Cowan, E. J. Chastain, D. A. Vilhena, J. S. Freudenberg, C. T. Bergstrom, Nodal dynamics, not degree distributions, determine the structural controllability of complex networks, PLoS ONE 7 (6) (2012) e38398. doi:10.1371/journal.pone.0038398.

[21] G. Li, H. Rabitz, Analysis of gene network robustness based on saturated fixed point attractors, EURASIP J. Bioinform. Syst. Biol. 2014 (4). doi:10.1186/1687-4153-2014-4.

[22] D. Angeli, J. E. Ferrel, Jr., E. D. Sontag, Detection of multistability, bifurcations, and hysteresis in a large class of biological positive-feedback systems, PNAS 101 (7) (2004) 1822–1827. doi:10.1073/pnas.0308265100.

[23] A. Tsoularis, J. Wallace, Analysis of logistic growth models, Math. Biosci. 179 (1) (2002) 21–55. doi:10.1016/S0025-5564(02)00096-2.

[24] M. Laurent, N. Kellershohn, Multistability: a major means of differentiation and evolution in biological systems, Trends Biochem. Sci. 24 (11) (1999) 418–422. doi:10.1016/S0968-0004(99)01473-5.

[25] W. L. Kath, J. D. Murray, Analysis of a model biological switch, SIAM J. Appl. Math. 45 (6) (1985) 943–955. doi:10.1137/0145057.

[26] A. Chatterjee, Y. N. Kaznessis, W.-S. Hu, Tweaking biological switches through a better understanding of bistability behavior, Curr. Opin. Biotechnol. 19 (5) (2008) 475–481. doi:10.1016/j.copbio.2008.08.010.

PeerJ PrePrints | http://dx.doi.org/10.7287/peerj.preprints.382v1 | CC-BY 4.0 Open Access | received: 8 May 2014, published: 8 May 2014

[27] J. J. Tyson, R. Albert, A. Goldbeter, P. Ruoff, J. Sible, Biological switches and clocks, J. R. Soc. Interface 5 (Suppl 1) (2008) S1–S8. doi:10.1098/rsif.2008.0179.focus.

[28] J. L. Cherry, F. R. Adler, How to make a biological switch, J. Theor. Biol. 203 (2) (2000) 117–133. doi:10.1006/jtbi.2000.1068.

[29] P. Smolen, D. A. Baxter, J. H. Byrne, Frequency selectivity, multistability, and oscillations emerge from models of genetic regulatory systems, Am. J. Physiol. 274 (1998) C531–C542.

[30] Q. Zhang, S. Bhattacharya, M. E. Andersen, Ultrasensitive response motifs: basic amplifiers in molecular signalling networks, Open Biol. 3 (2013) 130031. doi:10.1098/rsob.130031.

[31] M. E. Andersen, R. S. H. Yang, C. T. French, L. S. Chubb, J. E. Dennison, Molecular circuits, biological switches, and nonlinear dose-response relationships, Environ. Health Perspect. 110 (Suppl 6) (2002) 971–978.

[32] R. Ranaldi, S. Ferguson, R. J. Beninger, Automating the generation and collection of rate-frequency functions in a curve-shift brain stimulation reward paradigm, J. Neurosci. Methods 53 (2) (1994) 163–172. doi:10.1016/0165-0270(94)90174-0.

[33] B. D. Aguda, A. Friedman, Models of Cellular Regulation, Oxford University Press, NY, 2008.

[34] S. DeDeo, D. C. Krakauer, Dynamics and processing in finite self-similar networks, J. R. Soc. Interface (2012) (online)doi:10.1098/rsif.2011.0840.

[35] D. Siegal-Gaskins, M. K. Mejia-Guerra, G. D. Smith, E. Grotewold, Emergence of switch-like behavior in a large family of simple biochemical networks, PLoS Comput. Biol. 7 (5) (2011) e1002039. doi:10.1371/journal.pcbi.1002039.

[36] J. J. Tyson, B. Novak, Functional motifs in biochemical reaction networks, Annu. Rev. Phys. Chem. 61 (2010) 219–240. doi:10.1146/annurev.physchem.012809.103457.

[37] A. Mochizuki, An analytical study of the number of steady states in gene regulatory networks, J. Theor. Biol. 236 (3) (2005) 291 – 310. doi:10.1016/j.jtbi.2005.03.015.

[38] P. Brazhnik, A. de la Fuente, P. Mendez, Gene networks: how to put the function in genomics, Trends Biotechnol. 20 (11) (2002) 467–472. doi:10.1016/S0167-7799(02)02053-X.

PeerJ PrePrints | http://dx.doi.org/10.7287/peerj.preprints.382v1 | CC-BY 4.0 Open Access | received: 8 May 2014, published: 8 May 2014

[39] R. Milo, S. Shen-Orr, S. Itzkovitz, N. Kashtan, D. Chklovskii, U. Alon, Network motifs: Simple building blocks of complex networks, Science 298 (2002) 824–827. doi:10.1126/science.298.5594.824.

[40] M. Andrecut, Monte-carlo simulation of a multi-dimensional switch-like model of stem cell differentiation, in: C. J. Mode (Ed.), Applications of Monte Carlo Methods in Biology, Medicine and Other Fields of Science, InTech, 2011, Ch. 2, pp. 25–40. doi:10.5772/15474.

[41] B. D. MacArthur, C. P. Please, R. O. C. Oreffo, Stochasticity and the molecular mechanisms of induced pluripotency, PLoS ONE 3 (8) (2008) e3086. doi:10.1371/journal.pone.0003086.

[42] W. F. Boss, H. W. Sederoff, Y. J. Im, N. Moran, A. M. Grunden, I. Y. Perera, Basal signaling regulates plant growth and development, Plant Physiol. 154 (2) (2010) 439–443. doi:10.1104/pp.110.161232.

[43] T. Juven-Gershon, J. T. Kadonaga, Regulation of gene expression via the core promoter and the basal transcriptional machinery, Dev. Biol. 339 (2) (2010) 225–229. doi:10.1016/j.ydbio.2009.08.009.

[44] S. Goutelle, M. Maurin, F. Rougier, X. Barbaut, L. Bourguignon, M. Ducher, P. Maire, The hill equation: a review of its capabilities in pharmacological modelling, Fundam. Clin. Pharm. 22 (6) (2008) 633–648. doi:10.1111/j.1472-8206.2008.00633.x.

[45] M. Santillan, On the use of the hill functions in mathematical models of gene regulatory networks, Math. Model Nat. Phenom. 3 (2) (2008) 85–97. doi:10.1051/mmnp:2008056.

[46] J. X. Zhou, L. Brusch, S. Huang, Predicting pancreas cell fate decisions and reprogramming with a hierarchical multi-attractor model, PLoS ONE 6 (3) (2011) e14752. doi:10.1371/journal.pone.0014752.

[47] M. Chen, L. Wang, C. C. Liu, Q. Nie, Noise attenuation in the on and off states of biological switches, ACS Synth. Biol. 2 (10) (2013) 587–593. doi:10.1021/sb400044g.

[48] K. H. Kim, H. M. Sauro, Adjusting phenotypes by noise control, PLoS Comput. Biol. 8 (1) (2012) e1002344. doi:10.1371/journal.pcbi.1002344.

PeerJ PrePrints | http://dx.doi.org/10.7287/peerj.preprints.382v1 | CC-BY 4.0 Open Access | received: 8 May 2014, published: 8 May 2014

[49] S. Yamanaka, Elite and stochastic models for induced pluripotent stem cell generation, Nature 460 (2009) 49–52. doi:10.1038/nature08180.

[50] H. H. Chang, M. Hemberg, M. Barahona, D. E. Ingber, S. Huang, Transcriptome-wide noise controls lineage choice in mammalian progenitor cells, Nature 453 (2008) 544–548. doi:10.1038/nature06965.

[51] J. Wang, J. Zhang, Z. Yuan, T. Zhou, Noise-induced switches in network systems of the genetic toggle switch, BMC Syst. Biol. 1 (2007) 50. doi:10.1186/1752-0509-1-50.

[52] R. Dilao, The regulation of gene expression in eukaryotes: bistability and oscillations in repressilator models, J. Theor. Biol. (2014) (online)doi:10.1016/j.jtbi.2013.09.010.

[53] A. Kuznetsov, V. Afraimovich, Heteroclinic cycles in the repressilator model, Chaos Soliton. Fract. 45 (5) (2012) 660–665. doi:10.1016/j.chaos.2012.02.009.

[54] O. Buse, R. Perez, A. Kuznetsov, Dynamical properties of the repressilator model, Phys. Rev. E 81 (6) (2010) 066206. doi:10.1103/PhysRevE.81.066206.

[55] O. Purcell, N. J. Savery, C. S. Grierson, M. di Bernardo, A comparative analysis of synthetic genetic oscillators, J. R. Soc. Interface 7 (52) (2010) 1503–1524. doi:10.1098/rsif.2010.0183.

[56] S. Muller, J. Hofbauer, L. Endler, C. Flamm, S. Widder, P. Schuster, A generalized model of the repressilator, J. Math. Biol. 53 (6) (2006) 905–937. doi:10.1007/s00285-006-0035-9.

[57] M. B. Elowitz, S. Leibler, A synthetic oscillatory network of transcriptional regulators, Nature 403 (2000) 335–338. doi:10.1038/35002125.

[58] M. A. Leite, Y. Wang, Multistability, oscillations and bifurcations in feedback loops, Math. Biosci. Eng. 7 (1) (2010) 83–97. doi:10.3934/mbe.2010.7.83.

[59] N. Radde, The role of feedback mechanisms in biological network models, Asian J. Control 13 (5) (2011) 597–610. doi:10.1002/asjc.376.

[60] M. Mincheva, G. Craciun, Multigraph conditions for multistability, oscillations and pattern formation in biochemical reaction networks, P. IEEE 96 (8) (2008) 1281–1291. doi:10.1109/JPROC.2008.925474.

PeerJ PrePrints | http://dx.doi.org/10.7287/peerj.preprints.382v1 | CC-BY 4.0 Open Access | received: 8 May 2014, published: 8 May 2014

[61] D. Thieffry, Dynamical roles of biological regulatory circuits, Brief. Bioinform. 8 (4) (2002) 220–225. doi:10.1093/bib/bbm028.

[62] E. Bezout, Théorie générale des équations algébriques, Paris, Impr. de P.-D. Pierres, Paris, 1779.

[63] T. S. Macfarlan, W. D. Gifford, S. Driscoll, K. Lettieri, H. M. Rowe, D. Bonanomi, A. Firth, O. Singer, D. Trono, S. L. Pfaff, Embryonic stem cell potency fluctuates with endogenous retrovirus activity, Nature 487 (2012) 57–63. doi:10.1038/nature11244.

[64] S. Huang, Cell lineage determination in state space: A systems view brings flexibility to dogmatic canonical rules, PLoS Biol. 8 (5) (2010) e1000380. doi:10.1371/journal.pbio.1000380.

[65] C. H. Waddington (Ed.), The Strategy of the Genes, Geo Allen and Unwin, London, 1957.

[66] S. Masuda, J. Wu, T. Hishida, G. N. Pandian, H. Sugiyama, J. C. Izpisua Belmonte, Chemically induced pluripotent stem cells (cipscs): a transgene-free approach, J. Mol. Cell Biol. 5 (5) (2013) 354–355. doi:10.1093/jmcb/mjt034.

[67] P. Hou, Y. Li, X. Zhang, C. Liu, J. Guan, H. Li, T. Zhao, J. Ye, W. Yang, K. Liu, J. Ge, J. Xu, Q. Zhang, Y. Zhao, H. Deng, Pluripotent stem cells induced from mouse somatic cells by small-molecule compounds, Science 341 (6146) (2013) 651–654. doi:10.1126/science.1239278.

[68] G. N. Pandian, H. Sugiyama, Programmable genetic switches to control transcriptional machinery of pluripotency, Biotechnology Journal 7 (6) (2012) 798–809. doi:10.1002/biot.201100361.

[69] M. F. Pera, P. P. L. Tam, Extrinsic regulation of pluripotent stem cells, Nature 465 (2010) 713–720. doi:10.1038/nature09228.

[70] V. M. Weake, J. L. Workman, Inducible gene expression: diverse regulatory mechanisms, Nature Reviews Genetics 11 (2010) 426–437. doi:10.1038/nrg2781.

[71] R. Hanel, M. Pochacker, M. Scholling, S. Thurner, A self-organized model for cell-differentiation based on variations of molecular decay rates, PLoS ONE 7 (5) (2012) e36679. doi:10.1371/journal.pone.0036679.

PeerJ PrePrints | http://dx.doi.org/10.7287/peerj.preprints.382v1 | CC-BY 4.0 Open Access | received: 8 May 2014, published: 8 May 2014

[72] P. A. C. 't Hoen, M. Hirsch, E. J. d. Meijer, R. X. d. Menezes, G. J. van Ommen, J. T. d. Dunnen, mrna degradation controls differentiation state-dependent differences in transcript and splice variant abundance, Nucleic Acids Res. 39 (2) (2011) 556–566. doi:10.1093/nar/gkq790.

[73] J. Houseley, D. Tollervey, The many pathways of rna degradation, Cell 136 (2009) 763–776. doi:10.1016/j.cell.2009.01.019.

[74] R. Xu, M. A. J. Chaplain, F. A. Davidson, Modelling and analysis of a competitive model with stage structure, Math. Comput. Model. 41 (2-3) (2005) 159–175. doi:10.1016/j.mcm.2004.08.003.

[75] N. Suzuki, C. Furusawa, K. Kaneko, Oscillatory protein expression dynamics endows stem cells with robust differentiation potential, PLoS ONE 6 (11) (2011) e27232. doi:10.1371/journal.pone.0027232.

Appendix A. Examples of Oscillators

Appendix A.1. Repressilator in Example (2)

The network representation and matrix of the interaction coefficients of the CDM system in Example (2) are shown in Figure (A.10). Notice that one direction of inhibition is stronger than the reverse direction. This network is an example of a negative circuit forming a repressilator.

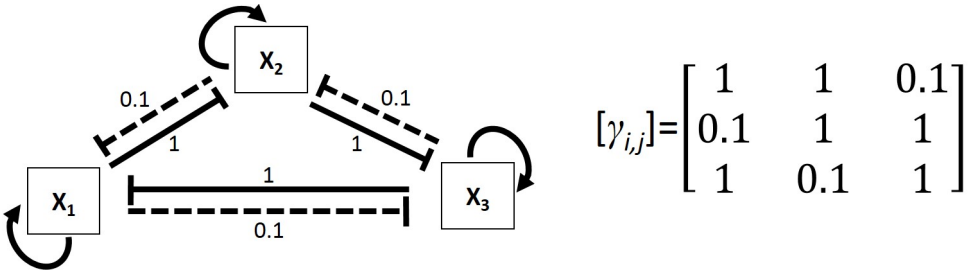

Figure A.10: Network representation and matrix of the interaction coefficients of the CDM system in Example (2). Solid bars represent strong inhibition, broken bars represent weak inhibition.

The CDM ODE model in Example (2) does not have stable steady states. In fact, there is only one steady state, $X^* = (5.693, 5.693, 5.693)$, but it is unstable. However, each component $X_i^* = 5.693$ is attracting. Property (1) cannot be used to determine the stability of this steady

PeerJ PrePrints | http://dx.doi.org/10.7287/peerj.preprints.382v1 | CC-BY 4.0 Open Access | received: 8 May 2014, published: 8 May 2014

state. Note that if the initial condition $X_{10} = X_{20} = X_{30}$, the solution converges to this sole steady state; but for other initial conditions, oscillations may persist.

Furthermore, the attracting components of every state contribute in the generation of the oscillating behavior (see Figure (A.11) for illustration).

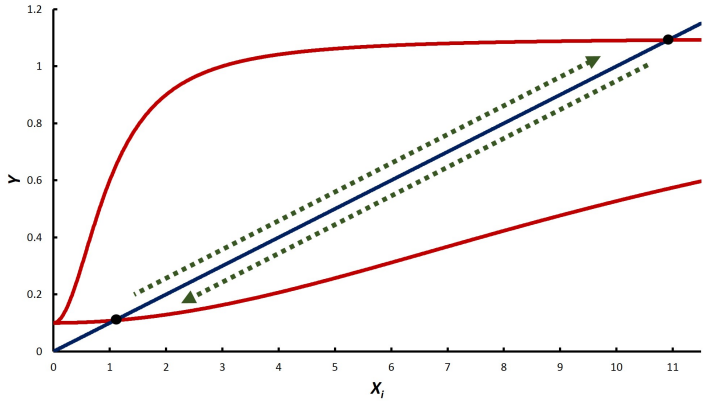

Figure A.11: The two sigmoid curves are sample graphs of $Y = H_i^1(X_i)$ with different values of X_j, $j \neq i$. The denominator of the sigmoid function H_i, $i = 1, 2, 3$ in the CDM model in Example (2) continuously varies resulting in oscillations. The oscillating solution to X_i is sequentially attracted by high-valued and low-valued attracting components.

Appendix A.2. CDM system with asymmetric matrix of inhibition exponents

Another example of an oscillator arising from the asymmetric inhibitory interaction of the components is of the following form

$$\begin{aligned}
\frac{dX_1}{dt} &= \frac{X_1^2}{1 + X_1^2 + X_2^3 + X_3} - 0.1X_1 + 0.1 \\
\frac{dX_2}{dt} &= \frac{X_2^2}{1 + X_1 + X_2^2 + X_3^3} - 0.1X_2 + 0.1 \\
\frac{dX_3}{dt} &= \frac{X_3^2}{1 + X_1^3 + X_2 + X_3^2} - 0.1X_3 + 0.1.
\end{aligned} \tag{A.1}$$

Notice that the matrix of inhibition exponents $[c_{i,j}]$ is asymmetric.

PeerJ PrePrints | http://dx.doi.org/10.7287/peerj.preprints.382v1 | CC-BY 4.0 Open Access | received: 8 May 2014, published: 8 May 2014

Appendix A.3. Stabilizing oscillations

Consider the following oscillating system

$$\begin{aligned}
\frac{dX_1}{dt} &= \frac{X_1^2}{1+X_1^2+X_2^2+0.1X_3^2} - 0.1X_1 + 0.1 \\
\frac{dX_2}{dt} &= \frac{X_2^2}{1+0.1X_1^2+X_2^2+X_3^2} - 0.1X_2 + 0.1 \\
\frac{dX_3}{dt} &= \frac{X_3^2}{1+X_1^2+\phi X_2^2+X_3^2} - 0.1X_3 + 0.1.
\end{aligned} \tag{A.2}$$

where $\phi = 0.1$ with initial condition $X_0 = (5, 1, 5)$. If we vary ϕ by setting

$$\frac{d\phi}{dt} = \frac{1}{1000(1+\phi^2)} \tag{A.3}$$

with initial value of ϕ equal to 0.1. This would lead to stabilized oscillation towards dominant X_2^* (Figure (A.12)).

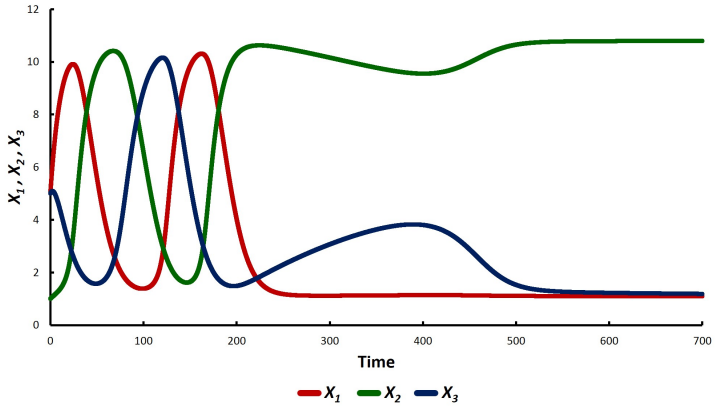

Figure A.12: An example of a controlled oscillating system by regulating an interaction coefficient.

Appendix B. Numerical results for Example (5)

The approximate values of the steady states of the ODE system (16) in Example (5) are

$(X_1^* = 18.619, X_2^* = 18.619)$ — stable (priming state),

$(X_1^* = 20.894, X_2^* = 3.1056)$ — unstable,

$(X_1^* = 3.1056, X_2^* = 20.894)$ — unstable,

$(X_1^* = 0.047741, X_2^* = 0.047741)$ — unstable,

$(X_1^* = 0, X_2^* = 0.047728)$ — unstable,

$(X_1^* = 0.047728, X_2^* = 0)$ — unstable,

PeerJ PrePrints | http://dx.doi.org/10.7287/peerj.preprints.382v1 | CC-BY 4.0 Open Access | received: 8 May 2014, published: 8 May 2014

$(X_1^* = 0, X_2^* = 20.952)$ — stable (premier state),

$(X_1^* = 20.952, X_2^* = 0)$ — stable (premier state), and

$(X_1^* = 0, X_2^* = 0)$ — stable (zero state).

If $g_1 = 0.5$ is introduced, the sole equilibrium is $(X_1^* = 31.479, X_2^* = 0)$.

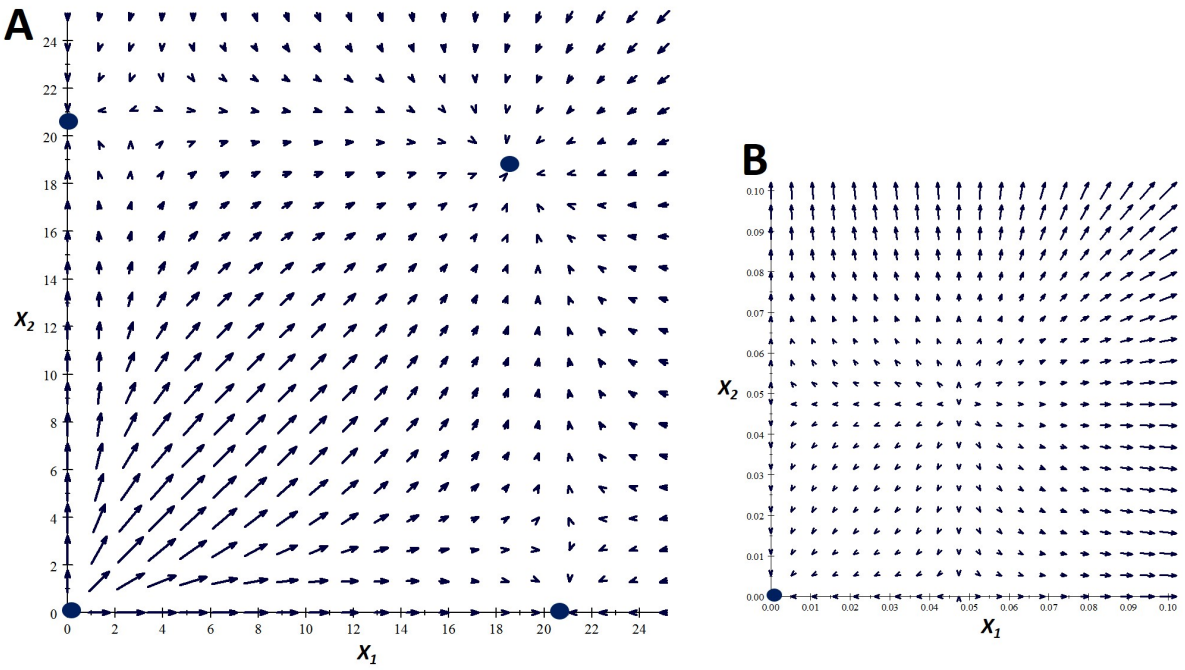

Figure B.13: (**A**) A phase plane showing the steady states of the ODE system (16) in Example (5), $g_1 = 0$. (**B**) Zooming in to show zero state is also stable.

PeerJ PrePrints | http://dx.doi.org/10.7287/peerj.preprints.382v1 | CC-BY 4.0 Open Access | received: 8 May 2014, published: 8 May 2014